Çagdas Topçu | Matthias Frühwirth | Maximilian Moser |
Michael Rosenblum | Arkady Pikovsky

Disentangling respiratory sinus arrhythmia in heart rate variability records

Physiological Measurement

IPEM Institute of Physics and Engineering in Medicine

PAPER

Disentangling respiratory sinus arrhythmia in heart rate variability records

Çağdaş Topçu[1,2], Matthias Frühwirth[3], Maximilian Moser[1,3] , Michael Rosenblum[2,4,5] and Arkady Pikovsky [2,4]

[1] Physiology, Otto Loewi Research Center for Vascular Biology, Immunology and Inflammation, Medical University of Graz, Neue Stiftingtalstr. 6/D05, A-8010 Graz, Austria
[2] Department of Physics and Astronomy, University of Potsdam, Karl-Liebknecht-Str. 24/25, D-14476 Potsdam-Golm, Germany
[3] Human Research Institute of Health Technology and Prevention Research, Franz Pichler Street 30, A-8160 Weiz, Austria
[4] The Research Institute of Supercomputing, Lobachevsky National Research State University of Nizhny Novgorod, Russia
[5] Author to whom any correspondence should be addressed.

E-mail: mros@uni-potsdam.de

Abstract

Objective: Several different measures of heart rate variability, and particularly of respiratory sinus arrhythmia, are widely used in research and clinical applications. For many purposes it is important to know which features of heart rate variability are directly related to respiration and which are caused by other aspects of cardiac dynamics. *Approach*: Inspired by ideas from the theory of coupled oscillators, we use simultaneous measurements of respiratory and cardiac activity to perform a nonlinear disentanglement of the heart rate variability into the respiratory-related component and the rest. *Main results*: The theoretical consideration is illustrated by the analysis of 25 data sets from healthy subjects. In all cases we show how the disentanglement is manifested in the different measures of heart rate variability. *Significance*: The suggested technique can be exploited as a universal preprocessing tool, both for the analysis of respiratory influence on the heart rate and in cases when effects of other factors on the heart rate variability are in focus.

1. Introduction

Heart rate variability (HRV) is a non-invasive measure of autonomic nervous system function. Therefore, its analysis and quantification are increasingly used in physiological and medical research, as well as in clinical practice. Typically, HRV denotes variation of the inter-beat intervals—defined in most cases as the intervals between the well-pronounced R-peaks in an electrocardiogram (ECG), and therefore called RR-intervals. A particularly important component of HRV is a modulation of the RR-intervals by respiratory influence, called respiratory sinus arrhythmia (RSA) (Katona and Jih 1975, Hirsch and Bishop 1981, Moser *et al* 1994, Hayano *et al* 1996, Billman 2011). RSA, the acceleration of heart rate during inspiration and deceleration during expiration, is thought to be a primarily vagally mediated oscillation originating from cardiovascular centers in the brain stem. These centers are in close proximity to respiratory centers and are synchronized with them (Lambertz and Langhorst 1998), especially during resting state, sleep and deep respiration. The physiological significance of RSA is, on one hand, in facilitating gas exchange between the lungs and the blood and thus helping the heart to do less work while maintaining optimal levels of blood gases (Larsen *et al* 2010, Ben-Tal *et al* 2012). On the other hand, another biological advantage of RSA is the stabilization of blood flow to the brain and the periphery by compensating arterial pressure changes arising from intrathoracic pressure changes due to ins- and expiration. It has been shown that blood pressure oscillations connected to respiration are reduced and the blood flow is thus stabilized by RSA (Elstad *et al* 2014). In medicine, the amplitude or the spectral power of RSA is used as a smart noninvasive measure for vagal tone (Moser *et al* 1994). The reason for this dominantly vagal origin of RSA can be found in the fast vagal synapses, able to quickly translate central respiratory oscillations present in

the brainstem to changes of cardiac sinus node discharge rate, which is not the case for the slow sympathetic synapses (Moser *et al* 2017).

Vagal tone is gaining importance in preventive and aging medicine, as the tone decreases with age (Lehofer *et al* 1999, Baylis *et al* 2013) and also because of chronic diseases connected to decreased vagal tone (Lehofer *et al* 1997). This understanding gained momentum when a vagal inflammatory reflex was discovered (Tracey 2002), indicating a close inverse connection between the available vagal tone and silent inflammation, a condition obviously resulting in chronic diseases like vascular sclerosis, Alzheimer's disease and cancer (see Nathan (2002) for a comprehensive overview). Since the accuracy of vagal tone determination by common time or frequency domain methods of RSA quantification—especially under conditions of different respiratory patterns—has been questioned (Laborde *et al* 2017), it is highly important to improve the methods for separation of respiratory and other influences of the autonomic nervous system on HRV.

A variety of data analysis techniques quantifying RSA have been proposed in the literature; for a discussion of commonly used metrics and their advantages and drawbacks, see e.g. Lewis *et al* (2012). Examples of application of RSA analysis include clinical psychology (Wielgus *et al* 2016), treatment of substance use disorder (Price and Crowell 2016), prediction of the course of depression (Panaite *et al* 2016), quantification of cardiac vagal tone and its relation to evolutionary and behavioral functions (Grossman and Taylor 2007) and quantification of vagal activity during stress in infants (Ritz *et al* 2012) and cancer patients (Moser *et al* 2006), to name just a few. On the other hand, quantification of the HRV component, not related to respiration, is important for the analysis of long-range and scaling properties of the cardiac dynamics (Ivanov *et al* 1999, Schmitt and Ivanov 2007).

In this paper, following our previous study (Kralemann *et al* 2013), we elaborate on a nonlinear technique that allows us to disentangle a respiratory-related component (R-HRV) from a component in which variability is caused by all other sources; we denote the latter component as NR-HRV. After the disentanglement, both components can be subject to any existing analysis technique. Thus, the suggested disentanglement can serve as a universal preprocessing tool that allows a researcher to concentrate on particular aspects of HRV: if the interest is in a respiratorily caused modulation of the heart rate, then it makes sense to work with the R-HRV component. Conversely, if the variation of the heart rhythm due to perturbations other than respiration is important, then it makes sense to cleanse the data of the component caused by respiration first, and then to analyze the NR-HRV component.

Separation of respiratory influences from HRV records has also been treated previously by various ad hoc techniques (Widjaja *et al* 2014, Kuo and Kuo 2016) such as adaptive filtering, least-mean-error fitting of power spectra, and principal component analysis. Our approach is based on an idea from nonlinear dynamics and coupled oscillator theory (Winfree 1980, Glass 2001, Pikovsky *et al* 2001, Strogatz 2003). Within this framework, we treat cardiovascular and respiratory systems as two interacting endogenous, self-sustained oscillators, which allows for a low-dimensional description of their dynamics in terms of phases. This description, in turn, provides the desired disentanglement and better quantification of the corresponding HRV components, as described below.

2. Methods

2.1. Theoretical background

We start with a general theory, briefly presenting a phase-based description of the dynamics of interacting oscillators. In the simplest case of an autonomous noisy periodic or weakly chaotic oscillator, the phase dynamics obeys

$$\dot{\varphi} = \omega + \zeta(t), \tag{1}$$

where φ and ω are the phase and the natural frequency of the system, and the noise term $\zeta(t)$ accounts for intrinsic fluctuations of the system parameters. If the system experiences influences from external sources (which may be either regular or not), then—according to dynamical perturbation theory (see e.g. Pikovsky *et al* (2001) for details)—the leading effect of the external forces $\eta_s(t)$, where $s = 1, 2, \ldots$, is in the modulation of the phase, which now obeys

$$\dot{\varphi} = \omega + \sum_s q_s[\varphi, \eta_s(t)] + \zeta(t). \tag{2}$$

Here, q_s are coupling functions describing the response to the corresponding perturbations. These functions account for the property that the susceptibility of an oscillator to external perturbations generally depends on its phase. Notice that the forces $\eta_s(t)$ can have arbitrarily complex time dependence—i.e. they can be periodic, chaotic or stochastic. We emphasize that equation (2) is valid for weak forcing, in the first approximation in ε, where small parameter ε is the characteristic amplitude of forcing. In the second approximation in ε, there may appear terms depending on several forces η_s.

Suppose now that one of the forces, say the first one, $\eta_1(t)$, and the corresponding coupling function q_1, are known, and other forces $\eta_s(t), s \neq 1$, are unknown. Then we can use equation (2) in order to represent the variations of the instantaneous frequency as a sum of two components,

$$\dot{\varphi} = \omega + q_1[\varphi, \eta_1(t)] + \xi(t), \tag{3}$$

where $q_1[\varphi, \eta_1(t)]$ describes solely the impact of the force $\eta_1(t)$ on the phase dynamics, while

$$\xi(t) = \dot{\varphi} - q_1[\varphi, \eta_1(t)] - \omega = \sum_{s \neq 1} q_s[\varphi(t), \eta_s(t)] + \zeta(t) \tag{4}$$

describes the cumulative effect of all other forces and of the intrinsic fluctuations. The representation by equation (3) plays a central role in our approach.

Now we specify the theory to cover the system of our interest—namely, the cardiovascular system. Schematic illustration of the approach is given in figure 1. In particular, we consider experiments where both cardiac and respiratory activities are monitored simultaneously, and the ECG and the respiratory signal—e.g. the air flow at the nose—are recorded. It is natural to represent these two endogenous rhythms as outputs of two interacting oscillatory systems, which can be characterized by their phases. As discussed in detail below, these phases can be estimated from data.

Denoting the phase and the natural frequency of the cardiac oscillator by φ and ω respectively, we write, similarly to (3):

$$\dot{\varphi} = \omega + q_R[\varphi, \eta_R(t)] + \xi(t), \tag{5}$$

where the subscript R stands for respiration, and η_R describes the effect of the respiration on the cardiac frequency. The term $\xi(t)$, like in equation (4), describes the effect on the cardiac phase of the physiological rhythms other than respiration, as well as of non-rhythmical, stochastic, external and intrinsic perturbations.

In practice, measurements of respiration rather often (and in our experiments, as well—see Kralemann *et al* (2013)) do not provide a proper magnitude of the corresponding force η_R, but only its phase $\psi(t)$. Thus, we assume that the forcing term due to respiration is a 2π-periodic function of the time-dependent respiratory phase ψ. So, we write $\eta_R(t) = S[\psi(t)] = S[\psi(t) + 2\pi]$, and replace the coupling function $q_R[\varphi, \eta_R(t)]$ in equation (5) with a phase-based coupling function $Q_R(\varphi, \psi)$, thus obtaining

$$\dot{\varphi} = \omega + Q_R(\varphi, \psi) + \xi(t). \tag{6}$$

In order to introduce the main idea of our paper, we postpone the discussion of how the terms in equation (6) can be obtained from data, and assume for the moment that they are already known. Next, we focus on a link between the phase dynamics description via equation (6) and the standard representation of the HRV via a sequence of the RR-intervals. We emphasize that the phase φ can be always introduced in such a way that

$$\varphi(t_k) = 2\pi k, \tag{7}$$

where t_k is the instant of the kth R-peak. If some other definition of the phase is used, rescaling and addition of a constant phase shift ensures property (7). Note also that the phase can equivalently be considered as a variable wrapped to the $[0, 2\pi)$ interval; in this representation, the phase achieves the value 2π and is immediately reset to zero at the instant of an R-peak appearance. Thus, knowledge of the phase evolution $\varphi(t)$ yields RR-intervals and thus fully determines the HRV.

Exploiting the representation (6), we now introduce two new phases. The first, φ_R, describes solely the effect of the respiration on the instantaneous cardiac frequency, and obeys
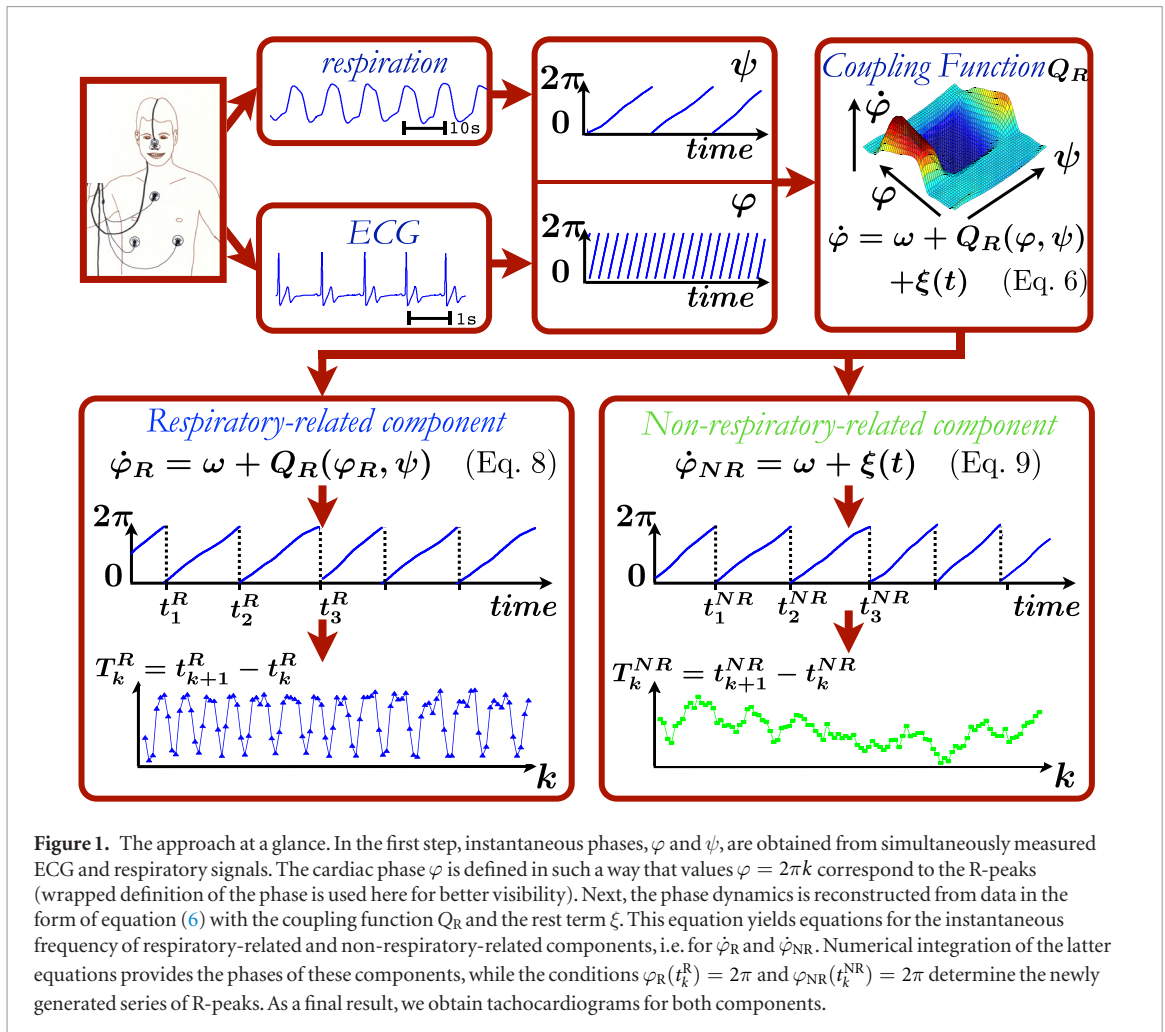
$$\dot{\varphi}_R = \omega + Q_R(\varphi_R, \psi). \tag{8}$$

This equation is obtained from equation (6) by dropping the last term. Correspondingly, the other phase, φ_{NR}, where the index *NR* stands for 'non-respiratory', describes the effect of all forces except for respiration, and of internal fluctuations, on the heart rate. This phase is governed by

$$\dot{\varphi}_{NR} = \omega + \xi(t). \tag{9}$$

In fact, because the time series $\varphi(t), \psi(t)$, and $\xi(t)$ are known from the processing of measured data, equations (8) and (9) can be straightforwardly integrated to yield time series $\varphi_R(t)$ and $\varphi_{NR}(t)$. (In practice, we used the Euler integration scheme with initial conditions $\varphi_R(t_1) = 0, \varphi_{NR}(t_1) = 0$.)

Knowing the phases φ_R, φ_{NR}, one can easily obtain the RR intervals via definition (7). The times at which the phase φ_R attains a value that is a multiple of 2π, i.e. when $\varphi_R(t_k^R) = 2\pi k$, yield a series of R-peaks, as it would appear in the presence of respiratory influence only (the superscript R stands for respiration). Thus, this series t_k^R and the corresponding series of RR-intervals $t_{k+1}^R - t_k^R$ represent the pure RSA-related component, R-HRV, of HRV. Conversely, if we are interested in the HRV due to all sources except for RSA, then we use the phase φ_{NR} to obtain the series of R-peaks, determined by the instants t_k^{NR}, such that $\varphi_{NR}(t_k^{NR}) = 2\pi k$, and the RR-intervals which vary due to non-respiratory influences only. This completes disentanglement of the R-HRV component,

Figure 1. The approach at a glance. In the first step, instantaneous phases, φ and ψ, are obtained from simultaneously measured ECG and respiratory signals. The cardiac phase φ is defined in such a way that values $\varphi = 2\pi k$ correspond to the R-peaks (wrapped definition of the phase is used here for better visibility). Next, the phase dynamics is reconstructed from data in the form of equation (6) with the coupling function Q_R and the rest term ξ. This equation yields equations for the instantaneous frequency of respiratory-related and non-respiratory-related components, i.e. for $\dot{\varphi}_R$ and $\dot{\varphi}_{NR}$. Numerical integration of the latter equations provides the phases of these components, while the conditions $\varphi_R(t_k^R) = 2\pi$ and $\varphi_{NR}(t_k^{NR}) = 2\pi$ determine the newly generated series of R-peaks. As a final result, we obtain tachocardiograms for both components.

given by the series of R-peaks at t_k^R and the series of interbeat intervals (tachocardiogram) $T_k^R = t_{k+1}^R - t_k^R$, from the NR-HRV component (the series t_k^{NR} and the corresponding tachocardiogram $T_k^{NR} = t_{k+1}^{NR} - t_k^{NR}$).

2.2. Reconstruction of the phase dynamics from data

We analyze, below, the set of 25 records of 420 s long simultaneous measurements of respiratory flow and ECG, already explored for different purposes in a previous publication (Kralemann *et al* 2013). The experiments were performed on healthy adults at rest, in a relaxed supine position, i.e. lying down with face up. To keep the measuremental noise as low as possible, we used bipolar, high-resolution recordings of respiration and ECG. The details of the measurements, the preprocessing and the subjects are described in the supplementary information to this paper and to Kralemann *et al* (2013).

Now, we describe the particular steps behind the general disentanglement approach presented above. Since the representation of the cardiac dynamics via equation (6) has been derived in Kralemann *et al* (2013), we outline the main steps only briefly here.

1. Recorded cardiac ECG signals and respiratory signals are embedded in a two-dimensional plane by virtue of the Hilbert transform. The protophase (phase-like variable) of the respiratory signal is obtained as an angle in this plane. The protophase of the ECG signal required an extended processing, because this signal has a complex form with several loops over a basic cycle. In fact, in these approaches, the details of parameterisation which may influence the definition of a protophase are not important, as is explained below.

2. A transformation from the protophases to the phases is performed, according to the method suggested in Kralemann *et al* (2008). The main idea is that because the embedding and the parameterisation of the embedded trajectory by a 2π-periodic phase-like variable are not unique, neither is the protophase obtained. The true phase is determined to have the property of growing linearly in time in the absence of external forces (see equation (1)—which is written for the true phase, so that the deterministic part of the r.h.s. does not depend on φ). We have performed an invertible deterministic transformation from the protophase to the phase (equation (4) in Kralemann *et al* (2013)), based on the property that the probability distribution density of the phase should be uniform.

Table 1. Summary of HRV measures and their descriptions.

Measures	Description	Reference
RMSSD (ms)	Root mean square of successive differences	Malik (1996)
logRSA	Logarithm of the median of the distribution of the absolute values of successive differences	Lehofer *et al* (1997)
pNN50	Relative number of successive pairs of RR-intervals, that differ by more than 50 ms	Malik (1996)
SDNN (ms)	Standard deviation of all (normal) RR intervals	Malik (1996)
VLF (ms^2)	Power of very low-frequency band (0.0033–0.04 Hz)	Malik (1996)
LF (ms^2)	Power of low-frequency band (0.04–0.15 Hz)	Malik (1996)
HF (ms^2)	Power of high-frequency band (0.15–0.4 Hz)	Malik (1996)
ApEn	Approximate entropy, complexity of RR intervals	Pincus *et al* (1991), Pincus (1991)
SampEn	Sample entropy, complexity of RR intervals	Richman and Moorman (2000), Chen *et al* (2009)

3. Having, now, the time series of the true phases of the cardiac system, $\varphi(t)$, and of the respiratory system, $\psi(t)$, we calculate the time derivative $\dot{\varphi}$ and fit it according to equation (6) with a function which is 2π-periodic in arguments φ, ψ. Practically, a kernel estimation (equation (7) in Kralemann *et al* (2013)) is employed to obtain $Q_R(\varphi, \psi)$, while the remaining terms of the fit provide time series ξ. As a result of this step, the basic equation (6) describing the cardiac phase dynamics is reconstructed.

2.3. Characterization of original and disentangled HRV data

In order to quantify the original RR-intervals and the results of the disentanglement procedure, we computed for all 25 data sets several physiologically relevant measures that are commonly used in HRV analysis. The overview of the measures used is given in table 1. We emphasize that the goal of the present study is not to compare the efficiency of the various standard measures, but to demonstrate that their values are affected by our disentanglement procedure—or, in other words, to demonstrate the relevance of our tool. This is why we have tried to implement our tests with as many different measures as possible. As we show below, some measures are more sensitive to this preprocessing than others. High sensitivity means that computation of the corresponding quantity after disentanglement allows for an essentially improved focus on a particular component of HRV.

Fifteen subjects without any cardiorespiratory disorder (9 M, 6 F, age 34.7 ± 7.3 yr, average interbeat interval 1027 ± 112 ms) participated in the experiments; for further details, see table I in the supplementary material (stacks.iop.org/PM/39/054002/mmedia). All subjects were presented with the detailed experimental protocol, which they had read and signed along with the informed consent approved by the research ethics committee of the Medical University of Graz and conforming to the Declaration of Helsinki.

2.3.1. Time-domain measures
The statistical measure in time-domain that directly characterizes the variability of the sequence of RR intervals is root mean square of successive differences (RMSSD) (Malik 1996), defined as

$$\text{RMSSD} = \sqrt{\langle (T_{k+1} - T_k)^2 \rangle_k},$$

where $\langle \cdot \rangle_k$ denotes averaging over k. Another measure is defined as the logarithm of the median of the distribution of the absolute values of successive differences (LogRSA) (Lehofer *et al* 1997), i.e.

$$\text{LogRSA} = \log \left[\text{median} |T_{k+1} - T_k| \right].$$

LogRSA accounts for a nearly log-normal statistical distribution of the medians, so that by taking logarithm a nearly normal distribution is achieved. Several studies (Lehofer *et al* 1997, 1999, Moser *et al* 1998, Grote *et al* 2007) have proven the robustness of LogRSA and its ability to differentiate between vagal states. Another characteristic of variability of RR interval series, used especially in clinical settings, is the relative number of successive pairs of RR-intervals that differ by more than 50 ms, denoted by pNN50 (Malik 1996). (Here, NN stands for the interval between normal, non-ectopic beats.) It is computed as the number of intervals such that $|T_{k+1} - T_k| > 50$ ms, divided by the total number of the RR intervals in the time series. Finally, we compute the standard deviation of RR intervals, SDNN.

2.3.2. Frequency-domain measures
In the frequency domain methods based on the power spectral density of the time series of RR intervals, one commonly computes the power in three frequency bands: VLF (very low frequency, from 0.0033 to 0.04 Hz), LF (low frequency, from 0.04 to 0.15 Hz) and HF (high frequency, from 0.15 to 0.4 Hz), e.g. by Fourier analysis. We

exploited for this purpose the procedure described in Clifford and Tarassenko (2005). The series of unevenly sampled RR intervals were interpolated and resampled at even time intervals of 1/7 s. The spectra were estimated using the Welch approach. A fast Fourier transform (FFT) was done on two signal sections of 300 s length after applying a Hamming window. The resulting periodograms were averaged, and the spectrum estimate numerically integrated over the frequency ranges defined above.

2.3.3. Nonlinear measures

Moreover, many nonlinear measures, mainly based on dynamical system approaches, have been applied to characterize HRV. Some of these measures require rather long time series, and are therefore not applicable to our relatively short observations. As appropriate indices, we have calculated the approximate entropy (ApEn) (Pincus *et al* 1991, Pincus 1991) and the sample entropy (SampEn) (Richman and Moorman 2000, Chen *et al* 2009) of the HRV time series. (The tolerance value was taken as 15% of the standard deviation and the embedding dimension was fixed at 2.) Summary of all HRV measures is given in table 1.

3. Results

3.1. Time series and spectra

First, we illustrate the method, presenting the original HRV series T_k along with the disentangled components T_k^R, T_k^{NR} in figures 2(a), (c), (e) and (g). In each panel, these three series are shown by different colors and markers, and additionally shifted vertically for better visibility. We have chosen these four characteristic cases for presentation, while all cases studied are presented in the supplementary material. In all 25 cases, the original HRV time series show different extent of interval-to-interval variability. The R-HRV time series also show significant variability; these time series are, however, much more homogeneous just by their construction: the term Q_R in equation (8) has a definite constant amplitude which is reflected in the magnitude of the variations of the R-HRV component. However, one can see clear differences in the NR-HRV series obtained via equation (9).

Basically, we can distinguish two types of NR-HRV data: 'smooth' and 'rough'. In the former case, the differences between successive RR intervals are small, and the whole graph looks like a curve, possibly slightly perturbed. Figure 2(g) is of this type. In the 'rough' case, the differences between the subsequent intervals are large, and one does not see a curve, but rather a dispersed set of points (panel (a)). There are also intermediate cases, as in panel (e). Finally, in panel (c), we show a remarkable NR-HRV pattern, consisting of 'smooth' patches interrupted nearly periodically (approx. at every 30th heart beat) by 'rough' bursts.

Complementary information is contained in the power spectra of the HRV records, shown in the right column of figure 2. One can clearly recognize several characteristic features:

1. The respiratory-related R-HRV component has pronounced peaks. These peaks can be interpreted as the main frequency of respiration and its harmonics.
2. The NR-HRV part contains no pronounced peak. This confirms that the main *regular* oscillatory contribution to the HRV is the respiration; all other perturbations are rather noisy, and do not exhibit noticeable spectral peaks (for the case depicted in panels ((c),(d)), the low-frequency periodicity cannot be resolved in the power spectrum for such a short time series).
3. The R-HRV component has low values at frequencies smaller than that of respiration. In fact, at these frequencies, the spectra of the original HRV and of the NR-HRV practically coincide. This means that the slow irregular variability of the heart rhythm is mainly caused not by respiration, but by other physiological processes. Our disentanglement allows one to study the time evolution of these slow components in a reliable way, by removing the respiratory component that may hide the interesting slow processes.

For another illustration of the disentanglement, we plot in figure 3 the original series and two constructed components versus time, i.e. $T_k = t_{k+1} - t_k$ versus t_{k+1}, $T_k^R = t_{k+1}^R - t_k^R$ versus t_{k+1}^R, and $T_k^{NR} = t_{k+1}^{NR} - t_k$ versus t_{k+1}^{NR}, for one data set. Here, we also show the time course of respiration, plotting $\cos \psi$ versus time. First, we see that the R-peaks in the HRV (filled circles) and in R-HRV (triangles) series occur at different instants of time. This naturally happens in case of any decomposition of HRV (peaks at the same instants would mean no decomposition at all). However, the overall pattern of the modulation by respiration, i.e. positions of peaks and troughs in the tachocardiograms, is preserved.

3.2. Time-domain characterizations of HRV

We now go beyond visual inspection of data and quantify the components according to the measures outlined in table 1.
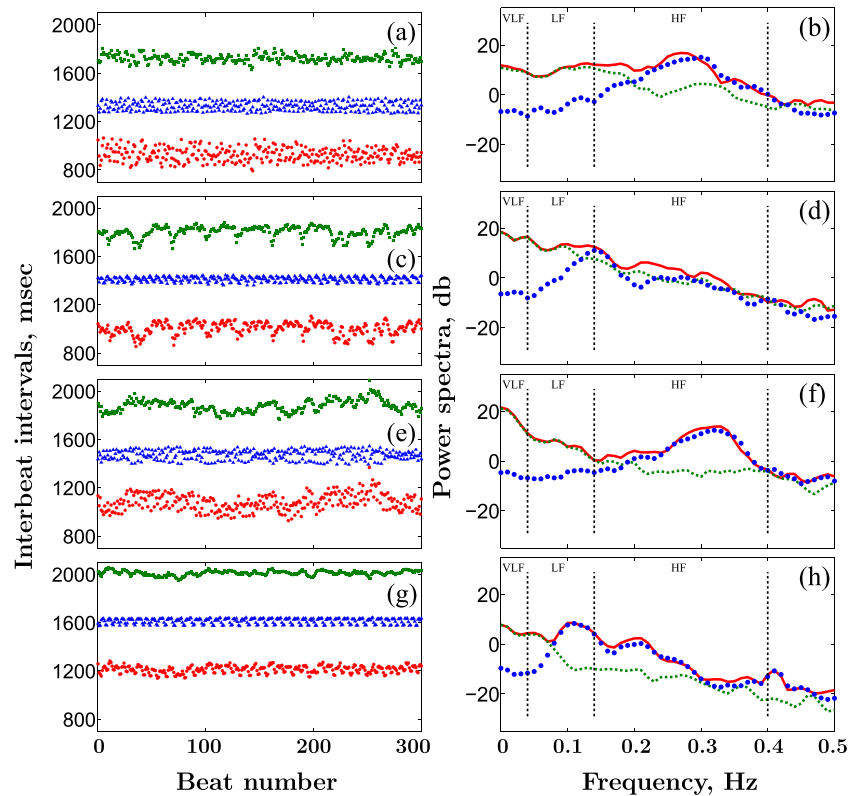
Figure 2. HRV plots (left column) and corresponding power spectral densities (right column). Original tachocardiogram (red circles) is shown along with its R-HRV (blue triangles) and NR-HRV components (green squares). The corresponding spectra are given by solid red, bold-dotted blue, and dotted green lines respectively. Left, for better visibility, RR intervals for the R-HRV component and for the NR-HRV component are shifted vertically by 400 ms and 800 ms respectively. For the same reason, only 300 beats are shown in the tachocardiograms; full records are shown in the supplementary material. In panels ((b), (d), (f), (h)), the domains of very low frequencies (VLF), low frequencies (LF), and high frequencies (HF) are separated by vertical dashed lines. For discussion, see text.
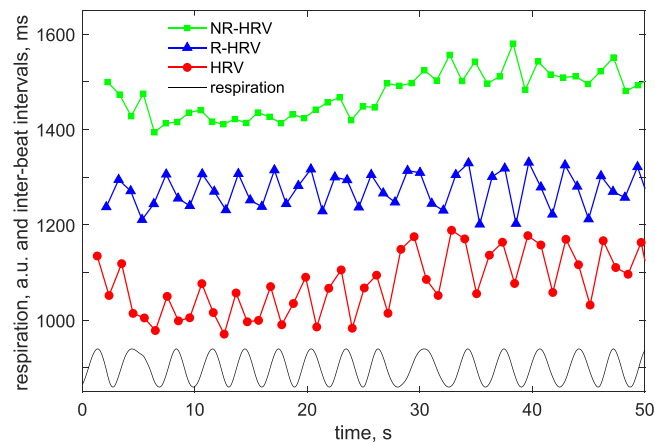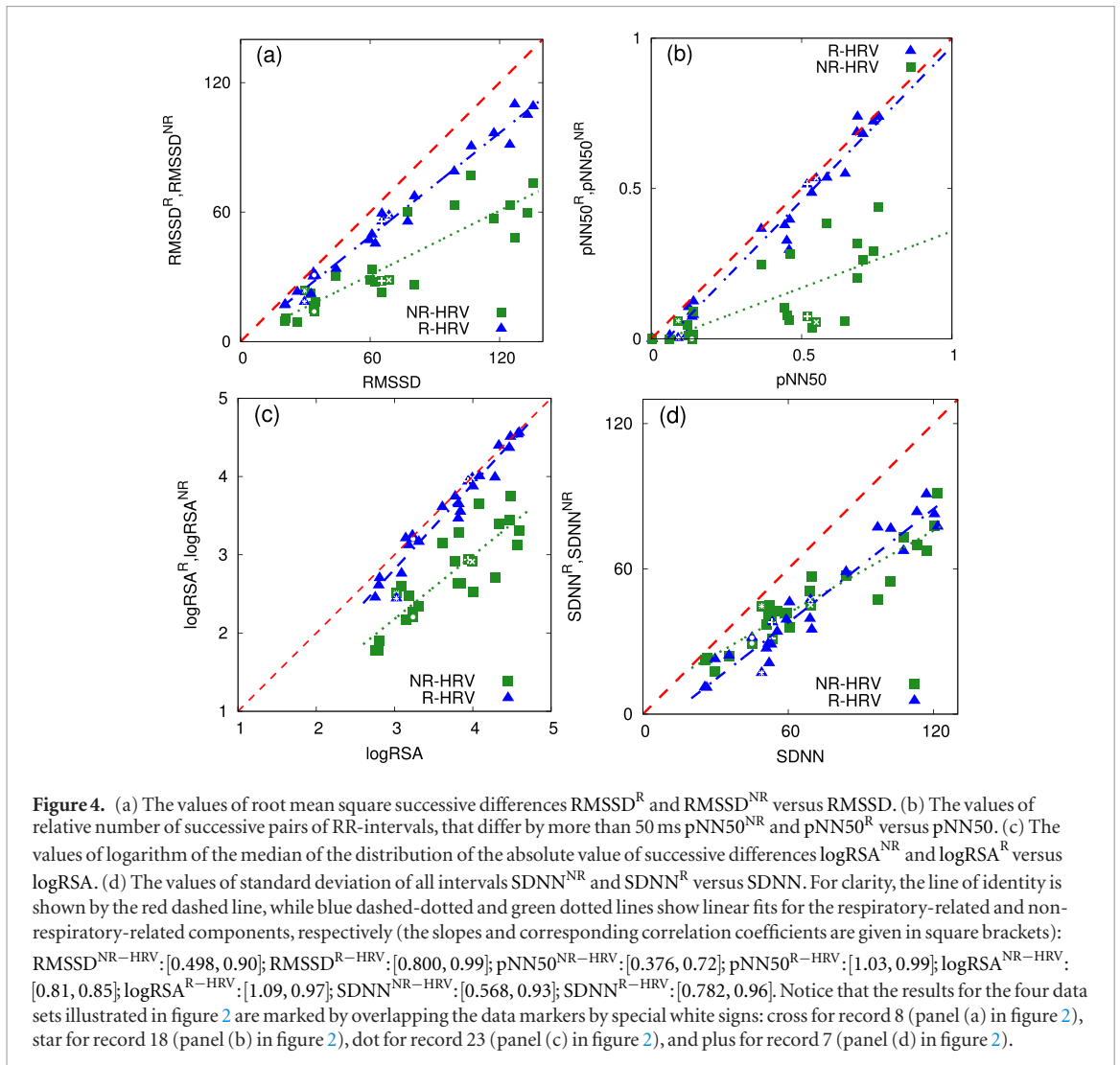

Figure 3. Example of the original HRV and its respiratory and non-respiratory related components. The latter two are shifted upwards for better visibility by 200 ms and 400 ms respectively. The black curve shows the respiratory signal with constant amplitude.

Figure 4(a) shows the RMSSD measure for both disentangled components of all data sets. We see that the RMSSD values for both the respiratory $RMSSD^R$ and non-respiratory $RMSSD^{NR}$ components are smaller than for the original one. We have found that in almost all cases, the reduction for the non-respiratory component is much stronger than for the respiratory one. One can see that the relative reduction of the RMSSD both for the R-HRV component (on average by factor 0.8) and NR-HRV component (on average by factor 0.5) does not depend on the RMSSD value for the original HRV series.

Panel (b) of the same figure presents the pNN50 measure of 'non-smoothness' of the RR interval series. One can see that this quantity is significantly reduced for the NR-HRV component, while its value for the R-HRV component is nearly the same as for the original data. (Excepted are cases where pNN50 in the original time series

Figure 4. (a) The values of root mean square successive differences RMSSD^R and RMSSD^{NR} versus RMSSD. (b) The values of relative number of successive pairs of RR-intervals, that differ by more than 50 ms pNN50^{NR} and pNN50^R versus pNN50. (c) The values of logarithm of the median of the distribution of the absolute value of successive differences logRSA^{NR} and logRSA^R versus logRSA. (d) The values of standard deviation of all intervals SDNN^{NR} and SDNN^R versus SDNN. For clarity, the line of identity is shown by the red dashed line, while blue dashed-dotted and green dotted lines show linear fits for the respiratory-related and non-respiratory-related components, respectively (the slopes and corresponding correlation coefficients are given in square brackets): RMSSD^{NR-HRV}: [0.498, 0.90]; RMSSD^{R-HRV}: [0.800, 0.99]; pNN50^{NR-HRV}: [0.376, 0.72]; pNN50^{R-HRV}: [1.03, 0.99]; logRSA^{NR-HRV}: [0.81, 0.85]; logRSA^{R-HRV}: [1.09, 0.97]; SDNN^{NR-HRV}: [0.568, 0.93]; SDNN^{R-HRV}: [0.782, 0.96]. Notice that the results for the four data sets illustrated in figure 2 are marked by overlapping the data markers by special white signs: cross for record 8 (panel (a) in figure 2), star for record 18 (panel (b) in figure 2), dot for record 23 (panel (c) in figure 2), and plus for record 7 (panel (d) in figure 2).

is very small—here, the successive pairs with RR intervals larger than 50 ms are nearly eliminated both in the R-HRV and NR-HRV components.)

Panel (c) in figure 4 shows the values of the LogRSA measure. Reduction of this measure in the NR-HRV component is even more evident than in panels ((a), (b)).

Finally, panel (d) demonstrates that the two components of the SDNN measure (the standard deviation of RR intervals) are reduced similarly.

3.3. Frequency-domain characterizations of HRV

The frequency-domain measures are plotted in figure 5. Here, we show the power in three frequency bands for R-HRV and NR-HRV series versus the corresponding powers of the original HRV (see dashed line which is the diagonal in the log–log representation). The VLF component (panel (a)) is strongly reduced in the R-HRV, while it is nearly the same as the original one in the NR-HRV. This is a clear indication that the VLF variability on time scales larger than 20 s is not due to respiration, but is caused by other physiological and external influences. However, the fine details of the VLF component are not very reliable, due to a shortness of the time series in our measurements.

In the LF range (time scales from roughly 25 to 6 s, panel (b)) the reduction in the R-HRV component is not so strong. In fact, for some subjects, the R-HRV component is even higher than the NR-HRV component. It is known from literature that slow respiration largely enhances HRV at six breaths per minute, where other LF rhythms coincide (Russo *et al* 2017). The HF range (panel (c), time scales from 6 to 2 s) includes a typical period of breathing. Therefore, here the situation is the opposite to the cases of lower frequencies: the respiration component is only slightly less than the original one, while the NR-HRV component is more reduced.

3.4. Complexity measures

Finally, we present the results of the computation of the complexity measures approximate entropy (ApEn) and sample entropy (SampEn). Both entropies show similar behavior: their values for both R-HRV and NR-HRV are smaller than the entropy values of the original HRV signals, which means that the complexity of the total HRV is
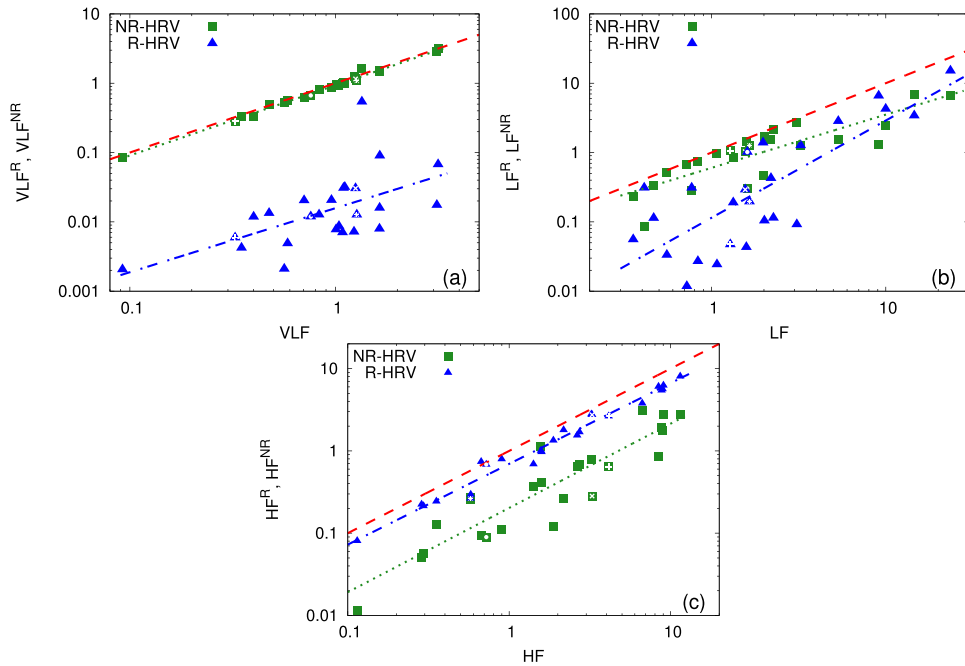
Figure 5. Spectral power in VLF (a), LF (b) and HF (b) spectral ranges. Here, the R-HRV and NR-HRV components are shown versus the value of the corresponding power in the original time series. The red dashed line shows the diagonal, i.e. the values for the original time series. Other dashed lines show the power law fits (the correlation coefficients for the fits are given in square brackets): $\text{VLF}^{\text{NR}-\text{HRV}} \approx 0.93 \cdot (\text{VLF})^{1.013}$ [0.97]; $\text{VLF}^{\text{R}-\text{HRV}} \approx 0.016 \cdot (\text{VLF})^{0.925}$ [0.58]; $\text{LF}^{\text{NR}-\text{HRV}} \approx 0.6 \cdot (\text{LF})^{0.768}$ [0.84]; $\text{LF}^{\text{R}-\text{HRV}} \approx 0.12 \cdot (\text{LF})^{1.40}$ [0.79]; $\text{HF}^{\text{NR}-\text{HRV}} \approx 0.20 \cdot (\text{HF})^{1.024}$ [0.91]; $\text{HF}^{\text{R}-\text{HRV}} \approx 0.70 \cdot (\text{HF})^{0.981}$ [0.99]. The results for the four data sets illustrated in Figure 2 are marked in the same way as in figure 4.
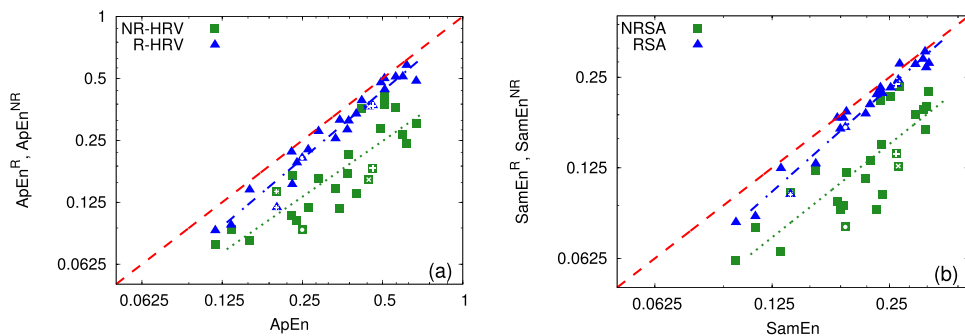

Figure 6. Values of the approximate entropy (a) and of the sample entropy (b) for the R-HRV and NR-HRV components, versus the values of these quantities in the original time series (red dashed line is the diagonal). Other dashed lines show the power law fits (the correlation coefficients for the fits are given in square brackets): $\text{ApEn}^{\text{R}} \sim (\text{ApEn})^{1.095}$ [0.98]; $\text{ApEn}^{\text{NR}} \sim (\text{ApEn})^{0.898}$ [0.84]; $\text{SampEn}^{\text{R}} \sim (\text{SampEn})^{1.15}$ [0.98]; $\text{SampEn}^{\text{NR}} \sim (\text{SampEn})^{1.03}$ [0.82]. One can see that for originally more complex signals (large values of SampEn and ApEn), reduction of complexity in the R-HRV component is smaller (the corresponding powers are larger than 1), but reduction in complexity in the NR-HRV component is larger (the powers are closer to 1). The results for the four data sets illustrated in Figure 2 are marked in the same way as in figure 4.

larger than that of its components. In almost all cases, the NR-HRV signal shows more regularity than the R-HRV component.

4. Conclusions and discussion

We have presented and illustrated a nonlinear technique which enables disentanglement of the RR-interval series into the respiratory-related component, R-HRV, and the remaining component, NR-HRV. The procedure can be performed if simultaneous measurements of an ECG and of a respiratory signal are available. Our method is based on the coupled oscillators model, and thus is inherently nonlinear. In particular, this means that our procedure is not a simple decomposition (in the sense of signal decomposition techniques)—i.e. R-HRV + NR-HRV $\neq$ HRV. The spectral analysis confirms the methodological validity of our approach, demonstrating that the R-HRV component correctly describes peaks in the power spectra at the respiratory-related frequencies. We suggest this approach be used as a universal preprocessing technique, allowing researchers

to concentrate on particular properties of the HRV data. Moreover, the technique can be used for investigation of other physiological rhythms if bivariate or multivariate measurements are available. We emphasize that equation (6) is also valid for nonstationary respiration or heart rate. However, the technique of coupling function reconstruction from data implies that this function remains unchanged within a certain time interval. Therefore, the disentanglement procedure will generally be performed in a running window. Numerical tests demonstrate that successful estimation of the coupling function is possible for data lengths of several hundred beats.

The results presented in figures 4–6 show that some HRV measures appear to be dominated by one of the components. So, figures 4(b) and (c) show that the values of LogRSA^R and of pNN50^R are very close to LogRSA and pNN50 respectively. In particular, this indicates that logRSA and pNN50 may be more efficient for quantification of the respiratory-related component than other measures, if no disentanglement is performed. However, pNN50 suffers from a saturation effect in subjects where HRV is generally low. Verification of this hypothesis requires further analysis with data from different groups of subjects. Moreover, figures 4–6 clearly demonstrate that computation of standard HRV measures from original data and its disentangled components generally yield different results, and this difference can be essential.

We summarize the results illustrated in figures 4–6 as follows. If a measure computed after disentanglement falls exactly on the line of identity, then the uncorrected measure truly reflects the respective component, i.e. in this particular case, the disentanglement can be omitted. Next, the respiratory component has been established as a reliable indicator of vagal tone, and it seems reasonable that the sympathetic activity is rather represented by the non-respiratory component of HRV. As the results show, the various time-domain, frequency domain and entropy measures reflect different components with a variable amount of inter-individual variance. This is reflected in different correlation coefficients. We consider a low inter-individual variance and a high correlation coefficient as indicators of a good representation of the respective components by the raw tachocardiogram. In contradistinction, a high variance and a low correlation coefficient would mark the measure based on raw data as less well suited to the representation of the respiratory or non-respiratory component of HRV. In this light, LogRSA and pNN50, as well as HF, most reliably represent the respiratory component and vagal tone, with pNN50 having the disadvantage of going into saturation at low values. The entropy measures in figure 6 give a less reliable representation of the respiratory component. On the other hand, VLF very closely represents the non-respiratory component, whereas LF does this only up to moderate values and with a much higher inter-individual variability. This results encourage the use of LogRSA and HF to noninvasively estimate vagal tone, and VLF to estimate sympathetic tone, whereas other investigated measures appear to be less well suited to the separation of the two components of autonomic nervous system activity.

We note that the technique requires rather high-quality ECG recordings and quite demanding preprocessing, related to the phase estimation. Therefore, we consider the current results a 'proof of principle'. A very useful practical improvement, now in progress, would be the development of an approximate disentanglement algorithm that can be performed on the basis of RR-series only—the latter being obtainable with any standard equipment. Another essential potential development would be to incorporate into the model the amplitude variations of the respiratory signal, modifying equation (6) to

$$\dot{\varphi} = \omega + A(t)Q(\varphi, \psi) + \xi(\varphi, t), \tag{10}$$

where $A(t)$ is the instantaneous amplitude, which can be extracted easily by means of the Hilbert transform. However, for this purpose, another type of measurement is required, in which the amplitude of the measured respiratory signal can be attributed to the true amplitude of the respiratory force affecting the cardiovascular system.

The new method promises an improved determination of vagal tone for medicine and prevention, based on an elaborated mathematical disentanglement of available data. It also allows for a better understanding of the non-respiratory components of HRV in general. The parasympathetic nervous system is an important part of our control center for silent inflammation (called the 'secret killer' in a *Time Magazine* communication (Gorman *et al* 2004) based on recent research (Das 2001, Tracey 2002, Nathan 2002, Baylis *et al* 2013)). Cellular receptors allowing communication between the autonomic nervous system and immune cells have been found in the past decade, and vagal activity has been proven to control immune activity (Tracey 2002, Nathan 2002). Therefore, a precise, noninvasive quantification of vagal tone will become important in several fields of medicine in the near future for diagnostic as well as therapeutic purposes. The method described in this paper might be a valuable contribution for such a highly desired accurate measurement tool. The level of vagal tone describes the ability of the organism to recover after inflammatory states, a property very important not only for our well-being and healthy aging, but for the prevention of serious chronic diseases like atherosclerosis, neurodegenerative diseases and cancer. Application of the method to medical diagnostics requires, however, future measurements from the corresponding groups of patients.

Finally, we mention that the suggested disentanglement technique can be used for other purposes, e.g. to quantify another manifestation of the cardio-respiratory interaction—namely, synchronization (Schäfer *et al* 1998). It is now established that degree of cardio-respiratory synchrony changes across physiological conditions, e.g. with age (Iatsenko *et al* 2013) or due to transition between different sleep states (Bartsch *et al* 2012). This measure has also been shown to be helpful in monitoring the transition between waking and anaesthetised states (Kenwright *et al* 2015). Furthermore, the disentanglement technique can be used as a universal preprocessing technique for analysis of other physiological rhythms, provided they can be modeled by coupled oscillatory systems. Hence, dynamical disentanglement could become an important tool in the emerging field of network physiology (Ivanov *et al* 2016).

Acknowledgments

ORCID iDs

Maximilian Moser ● https://orcid.org/0000-0001-9292-5091
Michael Rosenblum ● https://orcid.org/0000-0002-3044-6121
Arkady Pikovsky ● https://orcid.org/0000-0001-9682-7122

References

Bartsch R P, Schumann A Y, Kantelhardt J W, Penzel T and Ivanov P Ch 2012 Phase transitions in physiologic coupling *Proc. Natl Acad. Sci.* **109** 10181–6

Baylis D, Bartlett D B, Patel H P and Roberts H C 2013 Understanding how we age: insights into inflammaging *Longevity Healthspan* **2** 8

Ben-Tal A, Shamailov S S and Paton J F R 2012 Evaluating the physiological significance of respiratory sinus arrhythmia: looking beyond ventilation-perfusion efficiency *J. Physiol.* **590** 1989–2008

Billman G E 2011 Heart rate variability—a historical perspective *Front. Physiol.* **2** 86

Chen W, Zhuang J, Yu W and Wang Z 2009 Measuring complexity using FuzzyEn, ApEn, and SampEn *Med. Eng. Phys.* **31** 61–8

Clifford G D and Tarassenko L 2005 Quantifying errors in spectral estimates of HRV due to beat replacement and resampling *IEEE Trans. Biomed. Eng.* **52** 630–8

Das U N 2001 Is obesity an inflammatory condition? *Nutrition* **17** 953–66

Elstad M, Walløe L, Holme N L A, Maes E and Thoresen M 2014 Respiratory sinus arrhythmia stabilizes mean arterial blood pressure at high-frequency interval in healthy humans *Eur. J. Appl. Physiol.* **115** 521–30

Glass L 2001 Synchronization and rhythmic processes in physiology *Nature* **410** 277–84

Gorman C, Park A and Dell K 2004 The Secret Killer—The surprising link between inflammation and heart attacks, cancer, Alzheimer's and other diseases *Time Magazine* (February 23) pp 38–46

Grossman P and Taylor E W 2007 Toward understanding respiratory sinus arrhythmia: relations to cardiac vagal tone, evolution and biobehavioral functions *Biol. Psychol.* **74** 263–85

Grote V, Lackner H, Kelz C, Trapp M, Aichinger F, Puff H and Moser M 2007 Short-term effects of pulsed electromagnetic fields after physical exercise are dependent on autonomic tone before exposure *Eur. J. Appl. Physiol.* **101** 495–502

Hayano J, Yasuma F, Okada A, Mukai S and Fujinami T 1996 Respiratory sinus arrhythmia *Circulation* **94** 842–7

Hirsch J A and Bishop B 1981 Respiratory sinus arrhythmia in humans: how breathing pattern modulates heart rate *Am J Physiol.* **241** H620–9

Iatsenko D, Bernjak A, Stankovski T, Shiogai Y, Owen-Lynch P J, Clarkson P B M, McClintock P V E and Stefanovska A 2013 Evolution of cardiorespiratory interactions with age *Phil. Trans. R. Soc. Lond.* A **371** 8

Ivanov P Ch, Amaral L A N, Goldberger A L, Havlin S, Rosenblum M G, Struzik Z and Stanley H E 1999 Multifractality in human heartbeat dynamics *Nature* **399** 461–5

Ivanov P Ch, Liu K K L and Bartsch R P 2016 Focus on the emerging new fields of network physiology and network medicine *New J. Phys.* **18** 100201

Katona P G and Jih F 1975 Respiratory sinus arrhythmia: noninvasive measure of parasympathetic cardiac control *J. Appl. Physiol.* **39** 801–5

Kenwright D A *et al* 2015 The discriminatory value of cardiorespiratory interactions in distinguishing awake from anaesthetised states: a randomised observational study *Anaesthesia* **70** 1356–68

Kralemann B, Cimponeriu L, Rosenblum M, Pikovsky A and Mrowka R 2008 Phase dynamics of coupled oscillators reconstructed from data *Phys. Rev.* E **77** 066205

Kralemann B, Frühwirth M, Pikovsky A, Rosenblum M, Kenner T, Schaefer J and Moser M 2013 *In vivo* cardiac phase response curve elucidates human respiratory heart rate variability *Nat. Commun.* **4** 2418

Kuo J and Kuo Ch-D 2016 Decomposition of heart rate variability spectrum into a power-law function and a residual spectrum *Front. Cardiovasc. Med.* **3** 16

Laborde S, Mosley E and Thayer J F 2017 Heart rate variability and cardiac vagal tone in psychophysiological research—recommendations for experiment planning, data analysis and data reporting *Front. Psychol.* **8** 1–18

Larsen P D, Tzeng Y C, Sin P Y W and Galletly D C 2010 Respiratory sinus arrhythmia in conscious humans during spontaneous respiration *Respir. Physiol. Neurobiol.* **174** 111–8

Lambertz M and Langhorst P 1998 Simultaneous changes of rhythmic organization in brainstem neurons, respiration, cardiovascular system and EEG between 0.05 Hz and 0.5 Hz *J. Autonomic Nervous Syst.* **68** 58–77

Lehofer M, Moser M, Hoehn-Saric R, McLeod D, Liebmann P, Drnovsek B, Egner S, Hildebrandt G and Zapotoczky H G 1997 Major depression and cardiac autonomic control *Biol. Psychiatry* **42** 914–9

Lehofer M, Moser M, Hoehn-Saric R, McLeod D, Hildebrandt G, Egner S, Steinbrenner B, Liebmann P and Zapotoczky H G 1999 Influence of age on the parasympatholytic property of tricyclic antidepressants *Psychiatry Res.* **85** 199–207

Lewis G F, Furman S A, McCool M F and Porges S W 2012 Statistical strategies to quantify respiratory sinus arrhythmia: are commonly used metrics equivalent? *Biol. Psychol.* **89** 349–64

Malik M, Bigger J T, Camm J, Kleiger R E, Malliani A, Moss A J and Schwartz P J 1996 Heart rate variability: standards of measurement, physiological interpretation, and clinical use *Eur. Heart J.* **17** 354–81

Moser M, Frühwirth M, Messerschmidt D, Goswami N, Dorfer L, Bahr F and Opitz G 2017 Investigation of a micro-test for circulatory autonomic nervous system responses *Front. Physiol.* **8** 1–11

Moser M, Frühwirth M, Penter R and Winker R 2006 Why life oscillates—from a topographical towards a functional chronobiology *Cancer Causes Control* **17** 591–9

Moser M, Lehofer M, Hoehn-Saric R, McLeod D R, Hildebrandt G, Steinbrenner B, Voica M, Liebmann P and Zapotoczky H G 1998 Increased heart rate in depressed subjects in spite of unchanged autonomic balance? *J. Affective Disorders* **48** 115–24

Moser M, Lehofer M, Sedminek A, Lux M, Zapotoczky H G, Kenner T and Noordergraaf A 1994 Heart rate variability as a prognostic tool in cardiology. A contribution to the problem from a theoretical point of view *Circulation* **90** 1078–82

Nathan C 2002 Points of control in inflammation *Nature* **420** 846–52

Panaite V, Hindash A C, Bylsma L M, Small B J, Salomon K and Rottenberg J 2016 Respiratory sinus arrhythmia reactivity to a sad film predicts depression symptom improvement and symptomatic trajectory *Int. J. Psychophysiol.* **99** 108–13

Pikovsky A, Rosenblum M and Kurths J 2001 *Synchronization. A Universal Concept in Nonlinear Sciences* (Cambridge: Cambridge University Press)

Pincus S M 1991 Approximate entropy as a measure of system complexity *PNAS* **88** 2297–301

Pincus S M, Gladstone I M and Ehrenkranz R A 1991 A regularity statistic for medical data analysis *J. Clin. Monit.* **7** 335–45

Price C J and Crowell S E 2016 Respiratory sinus arrhythmia as a potential measure in substance use treatment—outcome studies *Addiction* **111** 615–25

Richman J S and Moorman J R 2000 Physiological time-series analysis using approximate entropy and sample entropy *Am. J. Physiol. Heart Circ. Physiol.* **278** H2039–49

Ritz T, Bosquet Enlow M, Schulz S M, Kitts R, Staudenmayer J and Wright R J 2012 Respiratory sinus arrhythmia as an index of vagal activity during stress in infants: respiratory influences and their control *PLoS One* **7** e52729

Russo M A, Santarelli D M and O'Rourke D 2017 The physiological effects of slow breathing in the healthy human *Breathe* **13** 298–309

Schmitt D T and Ivanov P Ch 2007 Fractal scale-invariant and nonlinear properties of cardiac dynamics remain stable with advanced age: a new mechanistic picture of cardiac control in healthy elderly *Am. J. Physiol.* **293** R1923–37

Schäfer C, Rosenblum M G, Kurths J and Abel H-H 1998 Heartbeat synchronized with ventilation *Nature* **392** 239–40

Strogatz S H 2003 *Sync: the Emerging Science of Spontaneous Order* (New York: Hyperion)

Tracey K J 2002 The inflammatory reflex *Nature* **420** 853–9

Widjaja D, Caicedo A, Vlemincx E, Van Diest I and Van Huffel S 2014 Separation of respiratory influences from the tachogram: a methodological evaluation *PLoS One* **9** 1–11

Wielgus M D, Aldrich J T, Mezulis A H and Crowell S E 2016 Respiratory sinus arrhythmia as a predictor of self-injurious thoughts and behaviors among adolescents *Int. J. Psychophysiol.* **106** 127–34

Winfree A T 1980 *The Geometry of Biological Time* (Berlin: Springer)